Video Article

Fluorescence-based Monitoring of PAD4 Activity via a Pro-fluorescence Substrate Analog

Mary J. Sabulski[1], Jonathan M. Fura[1], Marcos M. Pires[1]

[1]Department of Chemistry, Lehigh University

Correspondence to: Marcos M. Pires at map311@lehigh.edu

URL: http://www.jove.com/video/52114
DOI: doi:10.3791/52114

Keywords: Chemistry, Issue 93, PAD4, PADI4, citrullination, arginine, post-translational modification, HTS, assay, fluorescence, citrulline

Date Published: 11/5/2014

Citation: Sabulski, M.J., Fura, J.M., Pires, M.M. Fluorescence-based Monitoring of PAD4 Activity via a Pro-fluorescence Substrate Analog. *J. Vis. Exp.* (93), e52114, doi:10.3791/52114 (2014).

Abstract

Post-translational modifications may lead to altered protein functional states by increasing the covalent variations on the side chains of many protein substrates. The histone tails represent one of the most heavily modified stretches within all human proteins. Peptidyl-arginine deiminase 4 (PAD4) has been shown to convert arginine residues into the non-genetically encoded citrulline residue. Few assays described to date have been operationally facile with satisfactory sensitivity. Thus, the lack of adequate assays has likely contributed to the absence of potent non-covalent PAD4 inhibitors. Herein a novel fluorescence-based assay that allows for the monitoring of PAD4 activity is described. A pro-fluorescent substrate analog was designed to link PAD4 enzymatic activity to fluorescence liberation upon the addition of the protease trypsin. It was shown that the assay is compatible with high-throughput screening conditions and has a strong signal-to-noise ratio. Furthermore, the assay can also be performed with crude cell lysates containing over-expressed PAD4.

Video Link

The video component of this article can be found at http://www.jove.com/video/52114/

Introduction

A large number of mammalian proteins are heavily modified by the action of enzymes following the biosynthesis of proteins by the ribosome. These post-translational modifications (PTMs) can greatly increase the functional diversity of the proteome by changing the size, charge, structure, and oligomerization state (amongst other features) of proteins[1-3]. As a result, the change in protein structure can lead to physiological consequences, such as protein degradation, cellular differentiation, signaling, modulation in gene expression, and protein-protein interactions. While these modifications are prevalent in a large percentage of all human proteins, the terminal ends on histone proteins undergo an unusually high number of covalent modifications[4]. Histone proteins are a family of structural proteins that facilitate the condensation of genomic DNA. Covalent modifications of the unstructured histone tails are carried out and regulated by a series of enzymes that can catalyze the covalent modification of residues (writers), reverse the same modifications (erasers), and distinguish among the changes being imprinted onto the histone tails (readers)[5-7]. In fact, most of the known PTMs can be observed within this short segment of the histone including methylation, phosphorylation, acetylation, sumoylation, ubiquitination, and citrullination[8].

Citrullination involves the conversion of peptidyl-arginine to the non-*t*RNA encoded peptidyl-citrulline (**Figure 1A**). The proteins, responsible for this side chain neutralization, are members of the PAD (*p*eptide *a*rginine *d*eiminase) protein family, all of which are calcium-dependent enzymes.[9,10]. To date, five members of the PAD family have been described (PAD1, PAD2, PAD3, PAD4, and PAD6). Each member of this family appears to target distinct cellular proteins and also displays unique tissue distribution profiles. PAD4 is the only member of this protein family known to be localized within the nucleus via a nuclear localization sequence[11]. Accordingly, it has been shown to deiminate a number of nuclear targets, including arginine side chains on the N-terminal tails of histones H2A arginine residue 3 (H2R3), H3 (H3R2, H3R17, and H3R26) and H4 (H4R3)[12,13]. While each of the PAD isozymes have specific and critical physiological functions, PAD4 has received considerably more attention due to its role in a number of human processes in both diseased and healthy cells. Recently, PAD4 was shown to be a member of the pluripotency transcriptional network[14]. Both PAD4 expression levels and activity were shown to be elevated during reprogramming and ground-state pluripotent states in mice. By controlling the regulation of stem-cell genes, PAD4 may retain a pivotal role in cellular reprogramming efficiency. PAD4 has also been implicated in the formation of neutrophil extracellular traps, which upon binding of pathogens enable their system clearance. The hypercitrullination of histone proteins by PAD4 induces decondensation of the chromatin, which serves as the base material for the encapsulation of pathogenic bacteria by the extracellular trap, thus warding off bacterial infections[15,16].

Additionally, PAD4 has been found to play an active role in a number of human diseases. It has been previously shown that aberrant expression of PAD4 is associated with the onset and severity of rheumatoid arthritis, Alzheimer's, Parkinson's disease, and multiple sclerosis[17]. In fact, the presence of anti-citrullinated protein antibodies is one of the most reliable and definitive diagnostic and prognostic biomarkers of rheumatoid arthritis[18]. Likewise, dysregulated PAD4 activity has recently been observed in a number of human cancers including ovarian, breast, lung, and esophageal cancers[19-22]. The link between PAD4 and cancer has been shown to be mediated through the ELK1 oncogene or via the p53 tumor suppressor protein[22,23] and previous work has suggested that PAD4 could be a novel anti-cancer therapeutic target[17,24,25]. As a proof of principle

Copyright © 2014 Journal of Visualized Experiments

study, the depletion of PAD4 via shRNA in the colorectal cancer cell line HCT116 was revealed to be sufficient for inducing apoptosis and cell cycle arrest[26]. A recently developed irreversible PAD4 inhibitor led to a seventy percent reduction in tumor mass in mice[27]. Quite remarkably, PAD4 inhibition appeared to act as a targeted therapy that resulted in selective killing of cancerous cells while sparing untransformed cells.

The use of small molecules to turn off the function of PAD4 may prove to be a powerful new strategy to target cancer cells or to augment existing cancer chemotherapeutics[28]. Unfortunately, a potent reversible PAD4 inhibitor has yet to be discovered. A number of covalent inhibitors have been developed using the chloro/fluoro imidine handle that mimics the arginine substrate[27,29,30] and have proven to be practical tools in understanding the role of PAD4 in both healthy and diseased state cells. However, these molecules inhibit all of the active PADs with similar potency. Therefore, the need for a facile assay that reports on the activity of PAD4 is crucial. To date, PAD4 assays have been described that link the release of ammonia from the reaction to a colorimetric readout[31], utilize a fluorescently labeled chloroamidine substrate analog for fluorescence polarization assay[32], rely on the acid-assisted reaction between glyoxal and citrulline[33], and couple the PAD4 activity to a fluorescence dequenching step[34]. Of these, only the covalent modifier haloacetamidine strategy has proven to be compatible with high-throughput screening platforms[32,35,36]. We describe a facile fluorescence based assay that reliably measures the activity of PAD4. The assay, which displays a strong signal-to-noise ratio, speed of analysis, and robustness of measurement, has the potential to discover a truly potent and selective PAD4 inhibitor.

Protocol

1. PAD4 Transformation, Expression, and Purification

1. For PAD4 Transformation, transform the pGEX plasmid containing PAD4 GST fusion into chemically competent *E. Coli* (BL21(DE3)) cells for protein expression using the following procedure. Prepare chemically competent (calcium chloride) *E. Coli* (BL21(DE3)) cells according to standard protocols.
    1. Thaw 50 µl of previously prepared chemically competent BL21(DE3) cells on ice and mix with 1 µl of the pGEX plasmid containing PAD4 gene in a 5 ml culture tube. Incubate the mixture on ice for 10 min while gently shaking every 2 min.
    2. Heat shock the cells by placing the mixture in a 42 °C water bath for 40 sec. Immediately place the cell-plasmid mixture back on ice for 2 min to allow the cells to recover. Add 1 ml of sterile LB broth to the mixture and place on ice for 1 min.
    3. Incubate the heat shocked cells at 37 °C, shaking at 250 rpm for 1 hr. Pipette 75 µl of the transformed cells onto an ampicillin resistant agar plate and incubate at 37 °C for 15 hr. Store plate at 4 °C.

2. PAD4 Expression.
    1. Pick 1 colony of BL21(DE3) cells from the ampicillin agar plate and place in 5 ml of LB containing 1x ampicillin. Place in incubator and shake O/N at 37 °C.
    2. Transfer the 5 ml of LB (starter) into 1 L of sterile LB containing 1x ampicillin trihydrate (MW 403.45 g/mol). Place growth in a 37 °C shaking incubator. Monitor the OD_{600} of the growth. When growth reaches an OD_{600} of 0.3, move growth into 16 °C shaking incubator.
    3. Upon reaching an OD_{600} of 0.6, induce the cells with 0.3 mM isopropylthiagalactoside (IPTG, MW 238.30 g/mol). Allow cells to shake for 15 hr at 16 °C.
    4. Harvest cells by centrifugation at 4,000 x g for 20 min at 0 °C. Pour off supernatant and store pellet at -80 °C.

3. PAD4 Purification
    1. Re-suspend the pellet containing the expressed PAD4 in BL21(DE3) cells in a buffer of 50 mM NaCl (MW 58.44 g/mol), 300 mM NaH_2PO_4 (MW 119.98 g/mol), 10 mM Imidazole (MW 68.077 g/mol), 0.1 mM phenylmethylsulfonyl fluoride (PMSF, MW 174.94 g/mol) and 1 mM dithiothreitol (DTT, 154.25 g/mol), pH = 8.0.
    2. Lyse the cells via sonication for 15 min at 4 °C. Following sonication, centrifuge the cell lysate at 20,000 x g for 20 min at 0 °C. Pour off and save supernatant. Batch the supernatant with glutathione (GSH) agarose beads for 30 min at RT.
    3. Drain supernatant from GST beads/column via gravity. Wash beads with 4 x 25 ml of 1x PBS (phosphate buffered saline, pH = 8.0) at RT.
    4. Elute PAD4 with 2 x 10 ml Elution buffer, 50 mM tris (hydroxymethyl) aminomethane (Tris Base, MW 121.14 g/mol), 10 mM glutathione (GSH, MW 307.32 g/mol), pH = 8.0.
    5. Concentrate PAD4 using 100k MW cut-off centrifuge tubes and centrifuge at 4,000 x g for 20 min at 4 °C. Aliquot protein into 200 µl volumes in 1.0 ml microcentrifuge tubes and store at -80 °C.

2. Preparing Stock Solutions for Buffers

1. Weigh out sodium chloride (NaCl, MW 58.44 g/mol) and prepare a 2 M solution. Mix solution until clear.
2. Weigh out Tris(hydroxymethyl)aminomethane (Tris Base, MW 121.14 g/mol) and prepare a 2 M solution, pH = 8.0. Mix solution until clear.
3. Weigh out calcium chloride dihydrate ($CaCl_2$ $2H_2O$, MW 147.01 g/mol) and prepare a 500 mM solution. Mix solution until clear.
4. Weigh out Tris(2-carboxyethyl)phosphine (TCEP, MW 250.19 g/mol) and prepare a 200 mM solution. Mix solution until clear and store at -20 °C.
5. Weigh out dithiothreitol (DTT, MW 154.25 g/mol) and prepare a 1 M solution. Mix solution until clear and store at -20 °C.
6. Prepare a 0.5% solution of Triton X-100.
7. Weigh out ethylenediaminetetraacetic acid (EDTA, MW 292.24 g/mol) and prepare a 100 mM solution. Mix solution until clear.
8. Weigh out Z-Arg-Arg-7-amido-4-methylcoumarin hydrochloride (ZRcoum, MW 621.69 g/mol) and prepare a 10 mM solution in dimethyl sulfoxide (DMSO).

Copyright © 2014 Journal of Visualized Experiments

3. PAD4 Assay at 37 °C

1. From 10 mM ZRcoum stock, prepare a 125 µM solution of ZRcoum in water. This 125 µM ZRcoum solution will be Solution A.
2. Prepare a buffer of 62.5 mM NaCl, 62.5 mM Tris, 12.5 mM $CaCl_2$, 6.25 mM DTT, and 5 µM PAD4 (pH = 8.0). This will be Solution B.
3. Prepare a buffer of 62.5 mM NaCl, 62.5 mM Tris, 12.5 mM $CaCl_2$, and 6.25 mM DTT (pH = 8.0). This will be Solution C.
4. Weigh out Trypsin, crystalline (from bovine pancreas) and prepare a 10 mg/ml in 100 mM EDTA. Mix solution until clear and store at -20 °C. This will be Solution D.
5. Obtain a 96-well plate and designate a number of wells for controls (no PAD4) and test wells (+ PAD4).
6. Pipette 160 µl of Solution B into test wells and pipette 160 µl of Solution C into control wells. Incubate for 15 min at 37 °C.
7. Pipette 40 µl of Solution A into all wells and incubate at 37 °C for 45 min.
8. Pipette 10 µl of dH_2O to half of the control wells and half of the test wells. To the other half of control wells and test controls, pipette 10 µl of Solution D. Incubate for 10 min at 37 °C.
9. Obtain a fluorescence reading on a multimodal reader with an excitation wavelength of 345 nm and an emission wavelength of 465 nm.

4. PAD4 Assay at RT

1. From 10 mM ZRcoum stock, prepare a 50 µM solution of ZRcoum in water. This 50 µM ZRcoum solution will be Solution A.
2. Prepare a buffer of 100 mM NaCl, 100 mM Tris, 20 mM $CaCl_2$, 2 mM TCEP, 0.02% Triton X-100, and 8 µM PAD4 (pH = 8.0). This will be Solution B.
3. Prepare a buffer of 100 mM NaCl, 100 mM Tris, 20 mM $CaCl_2$, 2 mM TCEP, and 0.02% Triton X-100 (pH = 8.0). This will be Solution C.
4. Weigh out Trypsin, crystalline (from bovine pancreas) and prepare a 10 mg/ml in 100 mM EDTA. Mix solution until clear and store at -20 °C. This will be Solution D.
5. Obtain a 384-well plate and designate wells for controls (no PAD4) and test wells (+ PAD4).
6. Pipette 25 µl of Solution B into test wells and pipette 25 µl of Solution C into control wells. Allow buffer with/without PAD4 to incubate in wells for 20 min at RT.
7. Pipette 25 µl of Solution C into all wells and incubate for 45 min at RT.
8. Pipette 10 µl of dH_2O to half of the control wells and half of the test wells. To the other half of control wells and test controls, pipette 10 µl of Solution D. Incubate at RT for 10 min.
9. Obtain a fluorescence reading on a multimodal reader with an excitation wavelength of 345 nm and an emission wavelength of 465 nm.

5. PAD4 Time Course Assays at 37 °C and RT

1. From 10 mM ZRcoum stock, prepare a 125 µM solution of ZRcoum in water. This 125 µM ZRcoum solution will be Solution A.
2. Prepare a buffer of 62.5 mM NaCl, 62.5 mM Tris, 12.5 mM $CaCl_2$, 6.25 mM DTT, and 5 µM PAD4 (pH = 8.0). This will be Solution B.
3. Weigh out Trypsin, crystalline (from bovine pancreas) and prepare a 10 mg/ml in 100 mM EDTA. Mix solution until clear and store at -20 °C. This will be Solution C.
4. Obtain 2 96-well plates and pipet 160 µl of Solution B into # amount of wells (# of wells will depend on how many time points).
5. Incubate one 96-well plate at 37 °C. Incubate the other 96 well plate at RT.
6. Pipette 40 µl of Solution A into all wells in both 96-well plates and immediately pipette 10 µl of Solution C into the t = 0 min wells. Continue adding 10 µl of Solution C at specific time points until all wells have been quenched.
7. Obtain a fluorescence reading on a multimodal reader with an excitation wavelength of 345 nm and an emission wavelength of 465 nm.

6. PAD4 Inhibition Assay at RT

1. From 10 mM ZRcoum stock, prepare a 83 µM solution of ZRcoum in water. This 83 µM ZRcoum solution will be Solution A.
2. Weigh out Cl-amidine (MW 424.8 g/mol) and prepare a 100 µM stock solution. This will be Solution B.
3. Prepare a buffer of 100 mM NaCl, 100 mM Tris, 20 mM $CaCl_2$, 2 mM TCEP, 0.02% Triton X-100, and 8 µM PAD4 (pH = 8.0). This will be Solution C.
4. Prepare a buffer of 100 mM NaCl, 100 mM Tris, 20 mM $CaCl_2$, 2 mM TCEP, and 0.02% Triton X-100 (pH = 8.0). This will be Solution D.
5. Weigh out Trypsin, crystalline (from bovine pancreas) and prepare a 10 mg/ml in 100 mM EDTA. Mix solution until clear and store at -20 °C. This will be Solution E.
6. Obtain a 384-well plate and designate wells for controls (no PAD4), test wells (+ PAD4), and inhibition wells (PAD4 + Cl-amidine).
7. Pipette 25 µl of Solution C into test wells and pipette 25 µl of Solution D into control wells. Allow buffer with/without PAD4 to incubate in wells for 20 min at RT.
8. Pipette 10 µl of Solution B into inhibition wells and incubate for 20 min at RTe.
9. Pipette 15 µl of Solution A into all wells and incubate for 45 min at RT.
10. Pipette 10 µl of Solution E to all wells. Incubate at RT for 10 min.
11. Obtain a fluorescence reading on a multimodal reader with an excitation wavelength of 345 nm and an emission wavelength of 465 nm.

7. Crude Cell Lysate Assay at RT

1. After harvesting cells from PAD4 1 L growth, resuspend cells in 10 ml of 50 mM Tris, 50 mM NaCl, 0.1 mM phenylmethylsulfonyl fluoride (PMSF, MW 174.94 g/mol) and 1 mM dithiothreitol (DTT, 154.25 g/mol), pH = 8.0.
2. Lyse the cells via sonication for 15 min at 4 °C. Centrifuge the cell lysate at 20,000 x g for 20 min at 0 °C. Concentrate the clear supernatant to half the volume by centrifugation at 4,000 rpm at 4 °C using 100k MW cut-off centrifuge tubes.
3. From 10 mM ZRcoum stock, prepare a 250 µM solution of ZRcoum in water. This 250 µM ZRcoum solution will be Solution A.

Copyright © 2014 Journal of Visualized Experiments

4. Prepare a buffer of 100 mM NaCl, 100 mM Tris, 20 mM $CaCl_2$, and 2 mM TCEP (pH = 8.0). This will be Solution B.
5. Weigh out Trypsin, crystalline (from bovine pancreas) and prepare a 10 mg/ml in 100 mM EDTA. Mix solution until clear and store at -20 °C. This will be Solution C.
6. Obtain a black 384-well plate and designate wells for controls (no cell lysate) and test wells (+ cell lysate).
7. Pipette 100 µl of Solution B into all wells and pipette 60 µl of cell lysate into test wells. Incubate for 20 min at RT.
8. Pipette 40 µl of Solution A into all wells and incubate for 45 min at RT.
9. Pipette 10 µl of Solution C to all wells. Incubate at RT for 10 min.
10. Obtain a fluorescence reading on multimodal reader with an excitation wavelength of 345 nm and an emission wavelength of 465 nm.

Representative Results

Initially, it was demonstrated that **ZRcoum** can report on the activity of PAD4 in a 96-well plate format. Wells were incubated with the substrate **ZRcoum** and in the presence/absence of PAD4. Following an incubation period of 45 min at 37 °C, the fluorescence was measured with a 340/40 – 475/15 nm filter (**Figure 2A**). As expected, the fluorescence levels remained low as the fluorophore within **ZRcoum** (or the citrullinated **ZRcoum**) remained in the locked state. Upon addition of excess trypsin/EDTA to the solution, the fluorophores were liberated from **ZRcoum** but remained mostly unchanged in the presence of PAD4. The addition of EDTA is intended to assist in the cessation of the PAD4 reaction due to its ability to chelate the essential calcium ions. From these data, a 5.2-fold decrease in fluorescence output was observed in the presence of PAD4. Next, the compatibility of the newly developed assay with high-throughput screening platforms was demonstrated. It was of primary interest to analyze four reaction variables that would be most favorable for screening purposes (1) the further miniaturization of the assay volume (2) the possibility of performing the assay at RT (3) the stability of the protein and buffer mixture prior to completing the assay and (4) the potential interference of organic solvents/detergents.

For mid- or high-throughput screening efforts, high-density well plates are commonly utilized in small molecule screens. It was verified that the assay can be performed almost identically in a 384-well plate as compared to a 96-well plate (**Figure 2B**). In further determining the working conditions for the assay in a high-throughput format, it was important to investigate whether PAD4 activity can be monitored in a reasonable time frame at RT. Since not all liquid-handling instruments have a temperature controller, it can become cumbersome and costly to have an incubation step at elevated temperature. Furthermore, accounting for fluctuation in temperature can be a cause for discrepancy between plates and runs. In order to determine the effect of lower temperatures for the assay described here, a similar assay was performed at RT. It was found that the signals were virtually unchanged between 37 °C and RT (**Figure 3**). To further optimize the assay performance by minimizing the required incubation time between PAD4 and the substrate, the kinetics of the reaction was analyzed. PAD4 activity was monitored over time both at RT and 37 °C. As expected, it appears that PAD4 is more active at 37 °C (consistent with human physiological temperature) with the reaction mostly complete by 20 min. Satisfyingly, the reaction is not strongly affected by the reduction in temperature down to RT. The reaction proceeds at approximately half the speed as at the elevated temperature and is essentially complete 40-45 min post initiation. From the time course analyses, kinetics constants were calculated and the parameters (K_M = 397 µM, k_{cat} = 2.98 sec^{-1}, k_{cat}/k_M = 7,400 sec^{-1} M^{-1}) were found to be similar to other PAD4 substrates.[31] With the kinetics of the reaction characterized, all the subsequent assays were reduced to 1 hr from the beginning to the measuring point.

Next, stability of PAD4 was evaluated when dissolved in the reaction buffer over a prolonged period of time. Realistically, high-throughput screening will require reagents to be generally stable for many hours while the instrument is completing the screen. If certain reagents have a relative shelf-life of minutes, it can be quite expensive and time consuming to terminate the screen in order to prepare fresh reagents. Depending on the assay conditions, it is not unusual for some assays to be incompatible with high through-put screening for this very reason. With this idea in mind, the stability of PAD4 in buffer was monitored over several hours. Almost no loss in enzymatic activity was observed throughout the time period, thus indicating that the protein is stable even after sitting at RT for over 15 hr (**Figure 4A**). Next, it was evaluated whether the assay run under miniaturized conditions and at RT would still appropriately respond to the presence of a PAD4. Upon the incubation of the known PAD4 inhibitor, chloroamidine (Cl-amidine), led to a complete restoration of the fluorescence signal consistent with the full inhibition of PAD4 (**Figure 4B**). Finally, it was also verified that the presence of the organic solvent DMSO, commonly used in stock solutions of small molecules, up to 3% as final volume, did not interfere with the assay (data not shown). Likewise, the addition of 0.01% Triton X-100 resulted in similar fluorescence trends (data not shown).

Having shown that the assay is tolerant to a variety of conditions that are typically encountered in small molecule drug discovery efforts, a preliminary screening of 80 compounds was conducted and a robust Z' value of 0.71 was identified. In furthering the potential of the assay, the selectivity of the PAD4/**ZRcoum** reaction was highlighted by performing the reaction in crude whole cell lysates. *E. coli* cells containing the GST-PAD4 expression vector were induced with IPTG, similar to the procedure used for the isolation of GST-PAD4. Following the disruption of the cell membrane via sonication, the cellular debris was separated by centrifugation to afford a clarified cell lysate. When the PAD4-containing cell lysate was submitted to the same assay conditions as the purified GST-PAD4 assay, the fluorescence signal varied in agreement with the presence of active PAD4 in solution (**Figure 5**). Cell lysates contain a number of biomacromolecules at high concentrations that could potentially interfere with the activity of PAD4, the fluorescent properties of **ZRcoum**, and the trypsin step. The finding that the assay was functional in crude cell lysates indicates that there is a high selectivity in the reaction between PAD4 and **ZRcoum**. To further demonstrate that the signal decrease in the presence of crude cell lysates was specific to the presence of active PAD4, the effect of Cl-amidine, an established covalent PAD4 inhibitor, was evaluated. The addition of Cl-amidine led to a restoration in the fluorescence signal, consistent with the inactivation of PAD4 (**Figure 5**). Together, it was demonstrated the assay can be further simplified by utilizing crude cell lysates for the monitoring of PAD4 activity.

Copyright © 2014 Journal of Visualized Experiments

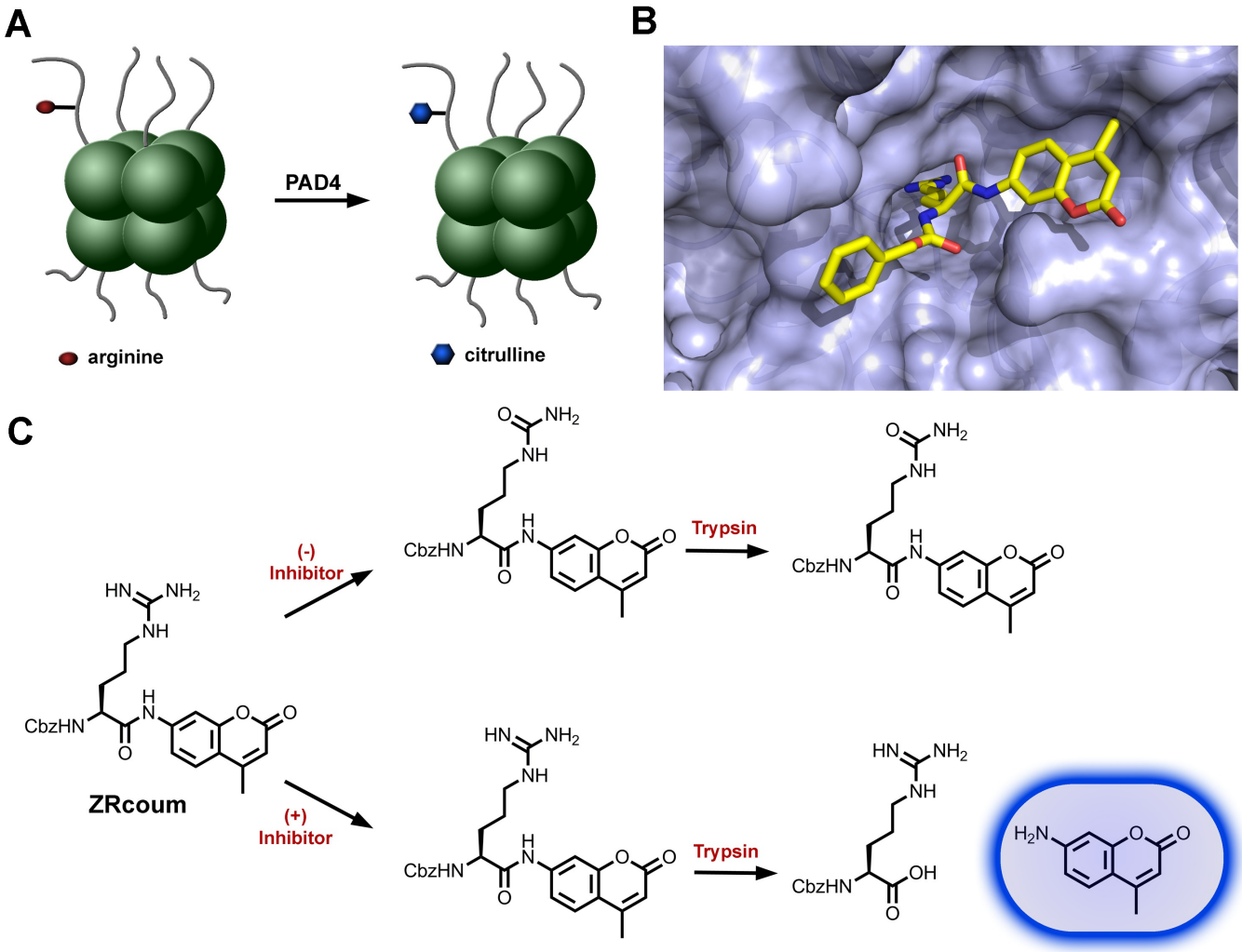

Figure 1. PAD4 and the design of its fluorescence-based assay. (**A**) Cartoon representation of the histone assemblies that make up the basic unit of a nucleosome. PAD4 catalyzes the citrullination of a number of arginine residues on histone proteins. (**B**) **ZRcoum** overlaid with the native substrate (hidden for clarity) of PAD4 (accession code 2DW5). (**C**) Representation of the steps in a typical PAD4 assay. Citrullination by PAD4 of the substrate **ZRcoum** reduces its susceptibility to trypsin-mediated amide hydrolysis, thus causing a change in fluorescence levels. Please click here to view a larger version of the figure.

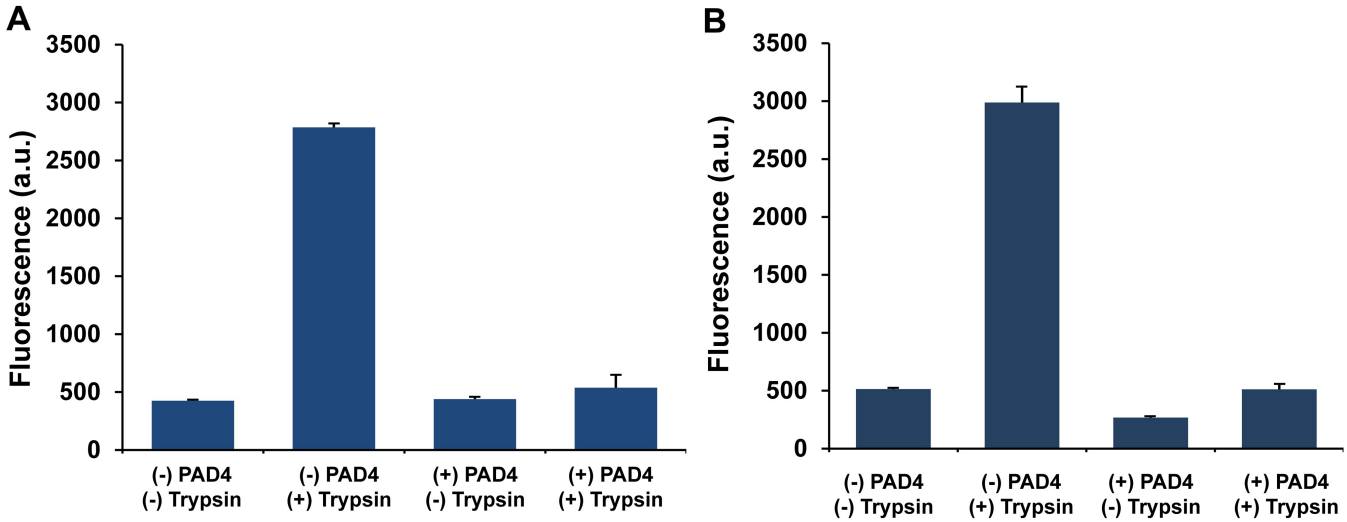

Figure 2. PAD4 assay in 96-well and 384-well plate formats. Fluorescence was measured (excitation 345 nm/emission 465 nm) in both a 96-well format (**A**) and 384-well format (**B**) with the designated conditions (37 °C). The addition of protease trypsin leads to a large increase in fluorescence levels in wells without PAD4 and remains virtually unchanged for wells with PAD4. Data are represented as mean + SD (*n* = 3). Please click here to view a larger version of the figure.

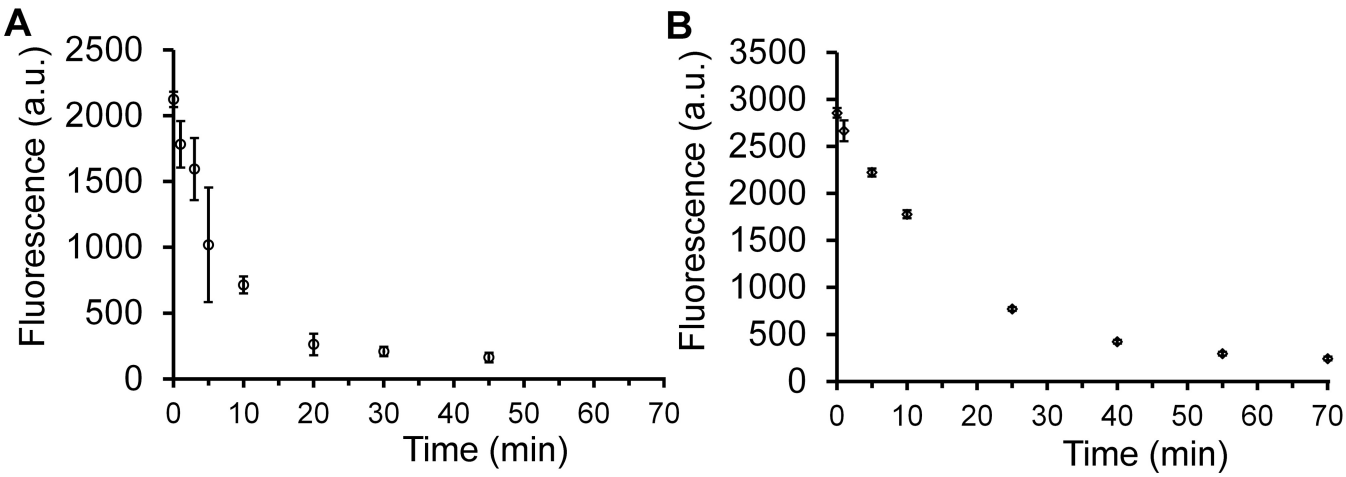

Figure 3. Time course analysis of PAD4 assay. Fluorescence was measured (excitation 345 nm/emission 465 nm) periodically in a 96-well plate format over 70 min with the protein being incubated either at 37 °C (**A**) or at RT (**B**). Data are represented as mean +/- SD (*n* = 3). Please click here to view a larger version of the figure.

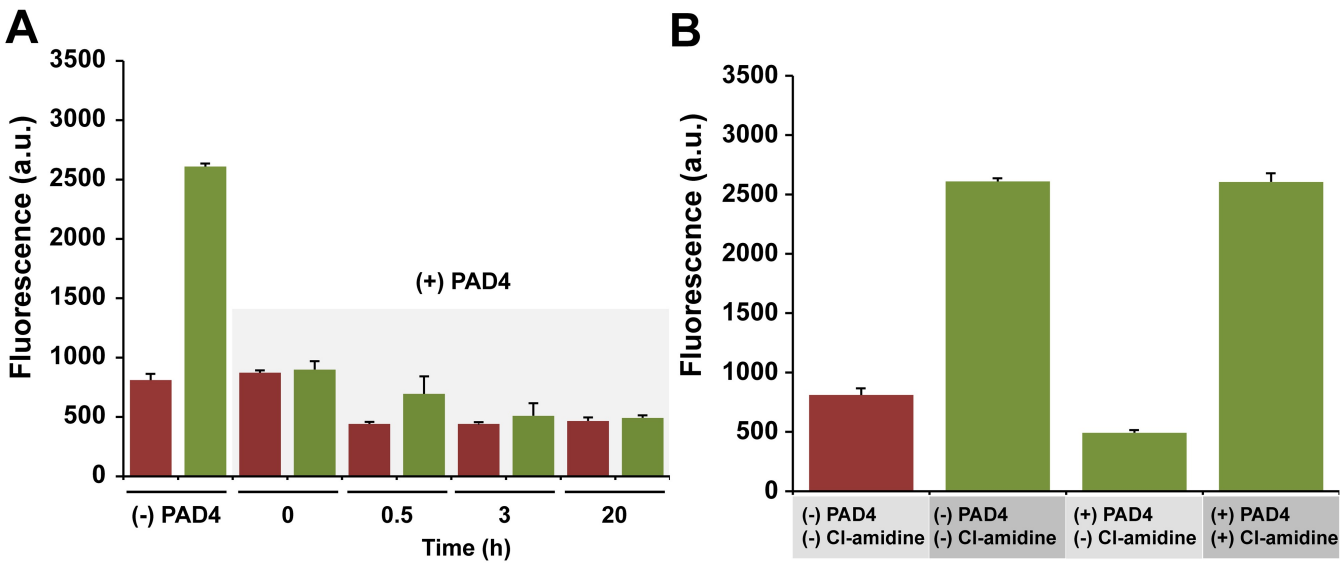

Figure 4. Protein stability and inhibition. (**A**) The activity of PAD4 was measured after the designated time intervals. For comparison, the fluorescence levels are shown in the absence of PAD4. Fluorescence levels are shown prior (red) and following (green) the addition of trypsin. (**B**) Introduction of the known PAD4 inhibitor Cl-amidine (100 μM) led to a restoration of the fluorescence signal in a 384-well plate format at RT. Fluorescence levels are shown prior (red) and following (green) the addition of trypsin. All data are represented as mean +/- SD (*n* = 3). Please click here to view a larger version of the figure.

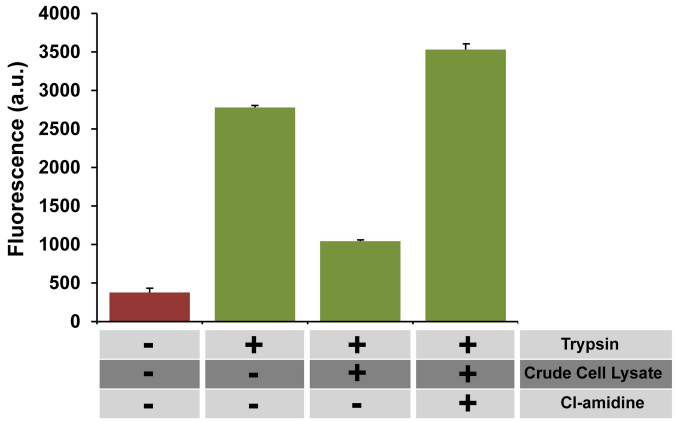

Figure 5. Crude cell lysate assay. The assay was performed in the absence and presence of crude cell lysates in a 384-well plate format at RT. Fluorescence levels are shown prior (red) and following (green) the addition of trypsin. Cl-amidine (100 μM) also caused an increase in fluorescence signal under these conditions. All data are represented as mean +/- SD (*n* = 3). Please click here to view a larger version of the figure.

Discussion

Herein, a fluorescence based assay was successfully developed that monitors the activity of PAD4. The assay has proven to be incredibly robust in a number of high-throughput conditions and is also compatible with whole cell lysates[37].

The affinity between the histone proteins and the DNA strands surrounding it loosens due the neutralization of the positive charge on the arginine side chain upon citrullination. It was envisioned that the neutralization of the arginine side-chain could be similarly leveraged to monitor PAD4 activity. The conversion of arginine to citrulline by PAD4 is expected to greatly reduce its susceptibility to trypsin-mediated hydrolysis. Trypsin has a distinct preference in hydrolyzing the C-terminal amide bonds of both lysine and arginine, with optimal activity near a pH range of 7.5 to 8.5. Thus, all trypsin solutions were prepared at a pH of 7.5 and all assays were conducted at a pH of 8.0. Furthermore, the acetylation of the fluorophore 7-amido-4-methylcoumarin onto the arginine C-terminus serves to “lock” its fluorescence in an off-state (**Figure 1C**). Upon treatment with trypsin, the 7-amido-4-methylcoumarin is uncoupled from the molecule, thus restoring its fluorescence. The change in fluorescence can be readily monitored in solution via its maximum excitation ~440 nm under physiological pH conditions. The enzymatic activity of PAD4 in converting arginine to citrulline should prevent the unmasking of the fluorophore, therefore reducing the fluorescence output. Additionally, the arginine amino terminus was acetylated as a carboxybenzyl moiety to mimic the native peptidic substrate, which lacks the charged amino group. The N-terminus acetylation was crucial since it has been previously reported that neither free arginine nor arginine-methyl ester is citrullinated by PAD4 to any appreciable levels[13]. This assay, in theory, could be used to monitor the activity of any of the five PAD isozymes. One limitation of the assay may be in cases where different isozymes are found within the same assay solution. All PAD isoforms could potentially convert **ZRcoum** to its citrulline counterpart. Therefore, selectivity between the isoforms is currently limited. Variations to the assay design in the future will involve the

inclusion of amino acids to the N-terminus of arginine. The elongation of the N-terminus may provide the substrate analog with higher selectivity by mimicking the native substrates.

Together, the pro-fluorescent PAD4 substrate analog Z-Arg-7-amido-4-methylcoumarin (**ZRcoum)** has the proper design features to allow for the monitoring of PAD4 activity. The introduction of the fluorophore to the C-terminal end of arginine within **ZRcoum** could, in theory, interfere with the ability of the molecule to be a substrate for PAD4. **ZRcoum** was found to be well accommodated within the binding pocket of PAD4 by analyzing its crystal structure whereby **ZRcoum** was docked into the known substrate binding pocket (PDB 2DW5)[38]. The coumarin fluorophore within **ZRcoum** appears to be well tolerated, an expected finding considering the substrate binding site is housed on a solvent exposed face of the protein (**Figure 1B**). A possible limitation of the assay as it pertains to the screening of small molecule libraries is that some potential inhibitors may display fluorescent properties that overlap with the fluorescence output from 7-amido-4-methylcoumarin. In this scenario, the fluorescent small molecule would result in a false positive signal. In the future, it is possible that the fluorophore moiety on the substrate analog could be varied to minimize this type of interference.

An additional unique feature of the assay compared to previously developed PAD4 assays is the increase in fluorescence levels due to the presence of a potential PAD4 inhibitor. To have an increase in fluorescence level (as opposed to a decrease) is a beneficial characteristic in terms of screening efforts as it renders the assay less susceptible to false positives. In conclusion, an operationally simple fluorescence-based assay was described for PAD4 activity by designing a pro-fluorescent substrate analog and it was shown that the assay is highly adaptable to conditions typically encountered in high-throughput screening platforms. This assay can be utilized in the future to possibly discover the first truly reversible PAD4 inhibitors.

Disclosures

The authors have nothing to disclose.

Acknowledgements

This work was supported by the Lehigh University Start-up Package. We thank Dr. Walter Fast for providing the GST-PAD4 plasmid for protein expression.

References

1. Jensen, O. N. Interpreting the protein language using proteomics. *Nat. Rev. Mol. Cell Biol.* **7**, 391-403, doi:10.1038/nrm1939 (2006).
2. Sims, R. J., 3rd, & Reinberg, D. Is there a code embedded in proteins that is based on post-translational modifications? *Nat. Rev. Mol. Cell Biol.* **9**, 815-820, doi:10.1038/nrm2502 (2008).
3. Pandey, A., & Mann, M. Proteomics to study genes and genomes. *Nature.* **405**, 837-846, doi:10.1038/35015709 (2000).
4. Berger, S. L. The complex language of chromatin regulation during transcription. *Nature.* **447**, 407-412, doi:10.1038/nature05915 (2007).
5. Fischle, W., Wang, Y., & Allis, C. D. Binary switches and modification cassettes in histone biology and beyond. *Nature.* **425**, 475-479, doi:10.1038/nature02017 (2003).
6. Taverna, S. D., Li, H., Ruthenburg, A. J., Allis, C. D., & Patel, D. J. How chromatin-binding modules interpret histone modifications: lessons from professional pocket pickers. *Nat. Struct. Mol. Biol.* **14**, 1025-1040, doi:10.1038/nsmb1338 (2007).
7. Seet, B. T., Dikic, I., Zhou, M. M., & Pawson, T. Reading protein modifications with interaction domains. *Nat. Rev. Mol. Cell Biol.* **7**, 473-483, doi:10.1038/nrm1960 (2006).
8. Strahl, B. D., & Allis, C. D. The language of covalent histone modifications. *Nature.* **403**, 41-45, doi:10.1038/47412 (2000).
9. Vossenaar, E. R., Zendman, A. J., van Venrooij, W. J., & Pruijn, G. J. PAD, a growing family of citrullinating enzymes: genes, features and involvement in disease. *Bioessays.* **25**, 1106-1118, doi:10.1002/bies.10357 (2003).
10. Gyorgy, B., Toth, E., Tarcsa, E., Falus, A., & Buzas, E. I. Citrullination: a posttranslational modification in health and disease. *Int. J. Biochem. Cell Biol.* **38**, 1662-1677, doi:10.1016/j.biocel.2006.03.008 (2006).
11. Nakashima, K., Hagiwara, T., & Yamada, M. Nuclear localization of peptidylarginine deiminase V and histone deimination in granulocytes. *J. Biol. Chem.* **277**, 49562-49568, doi:10.1074/jbc.M208795200 (2002).
12. Hagiwara, T., Hidaka, Y., & Yamada, M. Deimination of histone H2A and H4 at arginine 3 in HL-60 granulocytes. *Biochemistry.* **44**, 5827-5834, doi:10.1021/bi047505c (2005).
13. Kearney, P. L., *et al.* Kinetic characterization of protein arginine deiminase 4: a transcriptional corepressor implicated in the onset and progression of rheumatoid arthritis. *Biochemistry.* **44**, 10570-10582, doi:10.1021/bi050292m (2005).
14. Christophorou, M. A., *et al.* Citrullination regulates pluripotency and histone H1 binding to chromatin. *Nature*. **507** (7490), 104-8, doi:10.1038/nature12942 (2014).
15. Brinkmann, V., *et al.* Neutrophil extracellular traps kill bacteria. *Science.* **303**, 1532-1535, doi:10.1126/science.1092385 (2004).
16. Li, P., *et al.* PAD4 is essential for antibacterial innate immunity mediated by neutrophil extracellular traps. *J. Exp. Med.* **207**, 1853-1862, doi: 10.1084/jem.20100239 (2010).
17. Wang, Y., *et al.* Histone hypercitrullination mediates chromatin decondensation and neutrophil extracellular trap formation. *J. Cell. Biol.* **184**, 205-213, doi: 10.1083/jcb.200806072 (2009).
18. Wang, S., & Wang, Y. Peptidylarginine deiminases in citrullination, gene regulation, health and pathogenesis. *Biochim. Biophys. Acta.* **1829**, 1126-1135, doi: 10.1016/j.bbagrm.2013.07.003 (2013).
19. Trouw, L. A., & Mahler, M. Closing the serological gap: promising novel biomarkers for the early diagnosis of rheumatoid arthritis. *Autoimmun. Rev.* **12**, 318-322, doi:10.1016/j.autrev.2012.05.007 (2012).
20. Chang, X., & Fang, K. PADI4 and tumourigenesis. *Cancer Cell Int.* **10**, 7, doi:10.1186/1475-2867-10-7 (2010).
21. Wang, L., Chang, X., Yuan, G., Zhao, Y., & Wang, P. Expression of peptidylarginine deiminase type 4 in ovarian tumors. *Int. J. Biol. Sci.* **6**, 454-464 (2010).

Copyright © 2014 Journal of Visualized Experiments

22. Chang, X., *et al.* Investigating the pathogenic role of PADI4 in oesophageal cancer. *Int. J. Biol. Sci.* **7**, 769-781 (2011).
23. Zhang, X., *et al.* Genome-wide analysis reveals PADI4 cooperates with Elk-1 to activate c-Fos expression in breast cancer cells. *PLoS Genet.* **7**, e1002112, doi:10.1371/journal.pgen.1002112 (2011).
24. Tanikawa, C., *et al.* Regulation of histone modification and chromatin structure by the p53-PADI4 pathway. *Nat. Commun.* **3**, 676, doi:10.1038/ncomms1676 (2012).
25. Cui, X. *et al.* The induction of microRNA-16 in colon cancer cells by protein arginine deiminase inhibition causes a p53-dependent cell cycle arrest. *PLoS One.* **8**, e53791, doi:10.1371/journal.pone.0053791 (2013).
26. Jones, J. E., Causey, C. P., Knuckley, B., Slack-Noyes, J. L., & Thompson, P. R. Protein arginine deiminase 4 (PAD4): Current understanding and future therapeutic potential. *Curr. Opin. Drug Discov. Devel.* **12**, 616-627 (2009).
27. Li, P. *et al.* Regulation of p53 target gene expression by peptidylarginine deiminase 4. *Mol. Cell Biol.* **28**, 4745-4758, doi:10.1128/MCB.01747-07 (2008).
28. Wang, Y., *et al.* Anticancer peptidylarginine deiminase (PAD) inhibitors regulate the autophagy flux and the mammalian target of rapamycin complex 1 activity. *J. Biol. Chem.* **287**, 25941-25953, doi:10.1074/jbc.M112.375725 (2012).
29. Slack, J. L., Causey, C. P., & Thompson, P. R. Protein arginine deiminase 4: a target for an epigenetic cancer therapy. *Cell. Mol. Life Sci.* **68**, 709-720, doi:10.1007/s00018-010-0480-x (2011).
30. Luo, Y., Knuckley, B., Lee, Y. H., Stallcup, M. R., & Thompson, P. R. A fluoroacetamidine-based inactivator of protein arginine deiminase 4: design, synthesis, and *in vitro* and *in vivo* evaluation. *J. Am. Chem. Soc.* **128**, 1092-1093, doi:10.1021/ja0576233 (2006).
31. Knuckley, B., *et al.* Substrate specificity and kinetic studies of PADs 1, 3, and 4 identify potent and selective inhibitors of protein arginine deiminase 3. *Biochemistry.* **49**, 4852-4863, doi:10.1021/bi100363t (2010).
32. Knipp, M., & Vasak, M. A colorimetric 96-well microtiter plate assay for the determination of enzymatically formed citrulline. *Anal. Biochem.* **286**, 257-264, doi: 10.1006/abio.2000.4805 (2000).
33. Knuckley, B., *et al.* A fluopol-ABPP HTS assay to identify PAD inhibitors. *Chem. Commun.* **46**, 7175-7177, doi:10.1039/c0cc02634d (2010).
34. Bicker, K. L., Subramanian, V., Chumanevich, A. A., Hofseth, L. J., & Thompson, P. R. Seeing citrulline: development of a phenylglyoxal-based probe to visualize protein citrullination. *J. Am. Chem. Soc.* **134**, 17015-17018, doi:10.1021/ja308871v (2012).
35. Wang, Q., Priestman, M. A., & Lawrence, D. S. Monitoring of protein arginine deiminase activity by using fluorescence quenching: multicolor visualization of citrullination. *Angew. Chem. Int. Ed. Engl.* **52**, 2323-2325, doi:10.1002/anie.201208464 (2013).
36. Jones, J. E., *et al.* Synthesis and screening of a haloacetamidine containing library to identify PAD4 selective inhibitors. *ACS Chem. Biol.* **7**, 160-165, doi:10.1021/cb200258q (2012).
37. Dreyton, C. J., *et al. Optimization and characterization of a pan protein arginine deiminase (PAD) inhibitor.* doi:NBK148497 (2010).
38. Shimoyama, S., *et al.* Deimination stabilizes histone H2A/H2B dimers as revealed by electrospray ionization mass spectrometry. *J. Mass Spectrom.* **45**, 900-908, doi:10.1002/jms.1778 (2010).
39. Luo, Y., *et al.* Inhibitors and inactivators of protein arginine deiminase 4: functional and structural characterization. *Biochemistry.* **45**, 11727-11736, doi:10.1021/bi061180d (2006).

Copyright © 2014 Journal of Visualized Experiments